
This is an electronic reprint of the original article.
This reprint may differ from the original in pagination and typographic detail.

Author(s): Tarkiainen, R. & Ahlskog, M. & Paalanen, M. & Zyuzin, A. & Hakonen, Pertti J.

Title: Tunneling spectroscopy of disordered multiwalled carbon nanotubes

Year: 2005

Version: Final published version

Please cite the original version:

Tarkiainen, R. & Ahlskog, M. & Paalanen, M. & Zyuzin, A. & Hakonen, Pertti J. 2005. Tunneling spectroscopy of disordered multiwalled carbon nanotubes. *Physical Review B*. Volume 71, Issue 12. 125425/1-5. ISSN 1098-0121 (printed). DOI: 10.1103/physrevb.71.125425

Rights: © 2005 American Physical Society (APS). This is the accepted version of the following article: Tarkiainen, R. & Ahlskog, M. & Paalanen, M. & Zyuzin, A. & Hakonen, Pertti J. 2005. Tunneling spectroscopy of disordered multiwalled carbon nanotubes. *Physical Review B*. Volume 71, Issue 12. 125425/1-5. ISSN 1098-0121 (printed). DOI: 10.1103/physrevb.71.125425, which has been published in final form at <http://journals.aps.org/prb/abstract/10.1103/PhysRevB.71.125425>.

All material supplied via Aaltodoc is protected by copyright and other intellectual property rights, and duplication or sale of all or part of any of the repository collections is not permitted, except that material may be duplicated by you for your research use or educational purposes in electronic or print form. You must obtain permission for any other use. Electronic or print copies may not be offered, whether for sale or otherwise to anyone who is not an authorised user.

Tunneling spectroscopy of disordered multiwalled carbon nanotubes

R. Tarkiainen,* M. Ahlskog, M. Paalanen, A. Zyuzin,[†] and P. Hakonen
Low Temperature Laboratory, Helsinki University of Technology, FI-02015 HUT, Finland
 (Received 13 October 2004; published 28 March 2005)

The tunneling density of states has been studied on disordered multiwalled carbon nanotubes. The tunneling conductance shows a large zero-bias anomaly, whose temperature and voltage dependence is successfully compared with the non-perturbative theory of electron tunneling into a disordered 1D electrode. The environmental Coulomb blockade is expected to set in at lower energies, where junctions can be considered to be zero-dimensional. In one of the samples, Coulomb blockade behavior is revealed over a wide range of temperatures. In this sample the tunneling is also studied using a superconducting counterelectrode, and the observed reduction of the conductivity is found to be in quantitative agreement with the theory.

DOI: 10.1103/PhysRevB.71.125425

PACS number(s): 73.63.Fg, 73.40.Gk, 73.23.Hk

Measuring the tunneling conductance is a way to probe the effect of electron-electron interactions in carbon nanotubes.¹ Power law tunneling anomaly around zero bias has been observed in both single-walled² and multiwalled nanotubes.^{3–7} While in single-walled nanotubes Luttinger liquid is a valid model, in multiwalled nanotubes (MWNTs) the power law arises due to environmental modes compatible with LC -transmission line model.⁸ In a double junction configuration, when the samples are cooled down to low enough temperatures, complete Coulomb blockade develops both in single-walled⁹ and multiwalled nanotubes.^{10–12} In MWNTs the tunnel junctions are located between the metal electrodes and the nanotube, and the entire nanotube forms the island, where charge is localized.¹²

The above picture needs to be modified if the resistivity of the nanotubes is very high, or if the tunneling contacts have a finite size. In the diffusive electron transport limit, where the time it takes for the electron system to accommodate the tunneling charge becomes comparable to the time \hbar/eV , one observes the well known suppression of tunneling density of states near zero bias.¹³ Rollbühler *et al.*¹⁴ and Mishchenko *et al.*¹⁵ have calculated such anomalies nonperturbatively in infinite 1D junctions, and the former also considered the crossover from 1D to the 0D junction case, where tunneling can be described using the environmental quantum fluctuation theory (EQFT).¹⁶ In metallic systems the perturbative treatment is found sufficient,¹⁷ but disordered nanotubes allow one to reach the non-perturbative range experimentally. Measurements on boron-doped multiwalled nanotubes¹⁸ and bulk multiwalled nanotube samples¹⁹ showed deviations from the power law, pointing that this anomaly is relevant in disordered samples. Here we present observations and analysis of this type of behavior in individual disordered multiwalled nanotubes.

The power law anomalies have mainly^{3,5,6} been analyzed using the environmental Coulomb blockade theory,¹⁶ with an LC -transmission line modelling the carbon nanotube environment of the junction, which is assumed to be 0-dimensional. In this theory, the rate of inelastic tunneling is determined by the available electromagnetic modes of the environment, with which the tunneling electron can exchange energy. There is no explicit assumptions about the mean free path ℓ . When the resistivity of the nanotubes in-

creases, this model fails for two separate reasons. First of all, the power law is expected at the high energy regime $\epsilon = \max\{eV, k_B T\} \geq \hbar r/l$, where l and r are the transmission line parameters of the nanotube: r is the resistivity and l is the inductance per unit length. In the second place, one needs to have small enough contacts, $L_C < L_T^* = \sqrt{\hbar D^*}/\epsilon$, where L_C is the width of the contacts and $D^* = 1/rc_T$ is the field diffusion constant (c_T is the capacitance of the contact per unit length). This means that r needs to be low enough to leave some energy range available, e.g., $r \lesssim 1 \text{ k}\Omega/\mu\text{m}$. However in the present experiment, we are using nanotubes with $r = 30\text{--}100 \text{ k}\Omega/\mu\text{m}$, and both the assumption about the zero dimensionality of the contacts and the LC -line description of the environment will fail.

Our samples are made using CVD grown multiwalled nanotubes.²⁰ Previous studies have indicated that this material contains a large amount of defects,^{21,22} and the nanotubes have quite high resistivity, which we estimated from four-lead measurements as $r = 30\text{--}100 \text{ k}\Omega/\mu\text{m}$.²³ In a magnetic field, typical signature of 2D weak localization was observed, with phase coherence length $L_\phi \approx 10 \text{ nm}$, which is shorter than nanotube diameter. The temperature dependence of the conductivity was compatible with the interference and e - e interaction corrections in a 2D diffusive conductor, with very short ℓ .²¹ In order to access the tunneling density of states in these samples, the contact resistances need to be larger than $R_Q = h/e^2$, and clearly larger than the nanotube resistance. Partly, variation in G vs T arises from the change in nanotube conductivity, but as long as $R_{NT} \lesssim R_T$ this logarithmic change is small compared to the exponential suppression due to tunneling effects, and it shall be neglected in our analysis.

We chose to use aluminum as the contact material, because the contacts degrade quite fast by oxidation in air, creating a tunable contact resistance. For example, the two-terminal resistance of sample C increased from original $130 \text{ k}\Omega$ to $250 \text{ k}\Omega$ in roughly 2 days. Therefore we know that at room temperature the contact resistances $R_C > 60 \text{ k}\Omega/\text{contact}$, while the resistivity of the nanotube $\rho_{NT} \lesssim 50 \text{ k}\Omega/\mu\text{m}$. One of our samples, D, has Ti/Au contacts, and high contact resistances occurred accidentally. Main characteristics of our samples are given in Table I. All

TABLE I. Main characteristics of the samples. Φ is the diameter, L is the distance between the contacts, L_{total} is the total length of the nanotube, and L_C is the width of the contacts. Also resistance at 300 K is given.

Sample	Φ (nm)	L (μm)	L_{total} (μm)	L_C (μm)	$R_{300\text{ K}}$ (k Ω)
A	24	0.77	5.7	1.12/0.70	220 ^a
B	14	1.9	4.1	0.58/0.55	190
C	23	2.8	9	0.6/0.6	250
D	21	0.78	2.51	0.61/0.64	1600

^aMeasured at 1.3 K.

measurements were done in a 2-lead configuration.

The tunnel junctions can be considered 1D relative to field diffusion down to temperatures around $k_B T = \hbar D^* / L_C^2$. Below this temperature the system approaches the 0D Coulomb blockade limit. We have selected among the longest tubes and made the contacts relatively wide, 0.5–1.1 μm , in hoping to observe the 1D behavior over as large temperature scale as possible. Assuming $r = 50\text{ k}\Omega/\mu\text{m}$ and $c_T = 300\text{ aF}/\mu\text{m}$, we expect the one-dimensionality to be valid down to approximately 1 K. The width of the contacts and the large stray capacitance of a long nanotube should also guarantee that the total capacitance C_Σ is large enough so that the charging energy $E_C = e^2/2C_\Sigma \lesssim k_B T$, and to first approximation the charging effects can be considered small.

We have measured the differential conductance of our samples as a function of voltage and temperature. Figure 1(a) shows how conductance decreases when the samples are cooled down (a small magnetic field $B = 0.1\text{--}0.3\text{ T}$ was applied to keep the Al electrodes in the normal state). In these samples, it is not possible to describe the conductance by a single power law over the experimental range of temperatures. If the conductance is plotted on a $1/\sqrt{T}$ scale, as in Fig. 1(b), it becomes apparent that it is roughly given by $G \propto \exp(-\sqrt{T_0}/T)$, which is in accord with the nonperturbative result for tunneling into 1D disordered wires. Instead of the perturbative first order correction,¹³ $\delta\nu(\epsilon) \propto -\epsilon^{-1/2}$, one has tunneling density of states

$$\nu(\epsilon) = \nu_0 \left(1 - \text{erf} \sqrt{\frac{\epsilon^*}{\epsilon}} \right) \quad (1)$$

at $T = 0\text{ K}$ (Ref. 14) and

$$\nu(T) \sim \exp\left(-\sqrt{\frac{\epsilon^*}{k_B T}}\right) \quad (2)$$

at zero bias voltage, when $T \ll \epsilon^*$.¹⁵ At higher temperatures $\nu(\epsilon, T)$ can be obtained by numerical integration of Eq. (14) in Ref. 15, which is valid in the diffusive regime. The energy scale ϵ^* is given by¹⁴

$$\epsilon^* = \frac{e^2}{4c_T R_Q} r. \quad (3)$$

Using the density of states $\nu(\epsilon, T)$ one can calculate the conductance as

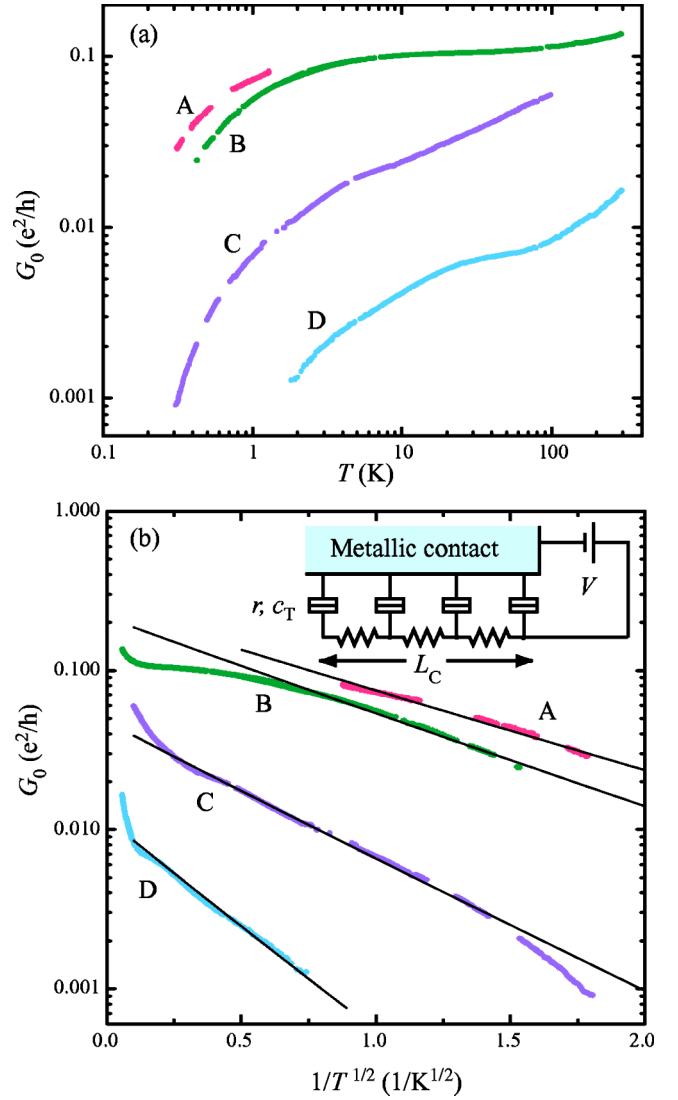


FIG. 1. (Color online) (a) Zero-bias conductance vs temperature. Normal state is induced in the Al electrodes by a small magnetic field (0.1–0.3 T). (b) Over a wide range of temperatures, the conductance is roughly given by $\log G \propto -1/\sqrt{T}$. The theoretical curves are calculated from the infinite 1D tunnel junction theory. The inset shows a schematic model of the tunneling system considered.

$$G(V, T) = \frac{1}{R_{\text{as}} \nu_0} \int d\epsilon \nu(\epsilon + eV, T) \frac{dn(\epsilon)}{d\epsilon}, \quad (4)$$

where $n(\epsilon)$ is the Fermi distribution. The full numerical calculation shows that the functional form of $G(T)$ differs only very slightly from $G \propto \exp(-\sqrt{T_0}/T)$. Fits to the experimental data are shown as solid lines in Fig. 1(b), and the corresponding parameters are given in Table II. The 1D junction model only has two adjustable parameters, ϵ^* and R_{as} .

To check if the model is reasonable, we assume a plausible value for the resistivity r of the nanotube, $50\text{ k}\Omega/\mu\text{m}$ for example, and extract a value for c_T from Eq. (3). We obtain $c_T = 140\text{--}950\text{ aF}/\mu\text{m}$, while in the literature values $540\text{ aF}/\mu\text{m}$ ¹² and $800\text{ aF}/\mu\text{m}$ (Ref. 11) have been reported

TABLE II. Fitting parameters of the 1D tunneling model. R_{as} is the resistance in the absence of the anomaly, i.e., at high voltages and/or temperatures. The ratio r/c_T has been calculated from ϵ^* .

Sample	R_{as} (k Ω)	ϵ^* (K)	r/c_T (k Ω /fF)
A	105	0.95	53
B	120	1.3	72
C	540	2.7	150
D	2200	6.6	370

for nanotube-metal contacts. Thus this model seems consistent.

The data in Table II suggest that there is a dependence between R_{as} and $\epsilon^* \propto r/c_T$. In Fig. 1(b) this is visible as a steeper slope for samples with higher resistance. As R_{as} is dominated by the tunneling resistance R_T , which mainly depends on the geometry of the junction, any variations in the intrinsic resistance of the nanotube r must be uncorrelated. It seems highly unlikely that any significant change in R_T would arise from some intrinsic property of the the nanotube, such as bare density of states, because R_T varies a lot even between different contacts on the same nanotube. The junction capacitance c_T on the other hand is inversely proportional to tunneling barrier width d , and assuming $R_T \propto \exp d$, we have $c_T \propto 1/\ln(R_T)$, which is compatible with the data. This observation suggests that the variation between samples mainly arises from the tunnel barrier, while all the nanotubes have similar r .

Theory also describes the suppression of tunneling at Fermi level as a function of bias voltage.¹⁴ In Fig. 2 the differential conductance of sample A at two different temperatures is compared to the theoretical prediction. The parameters ϵ^* and R_{as} from Table II are used in the calculation, with no additional fitting parameters. Since we know from 3-probe measurements that one of the junctions has much

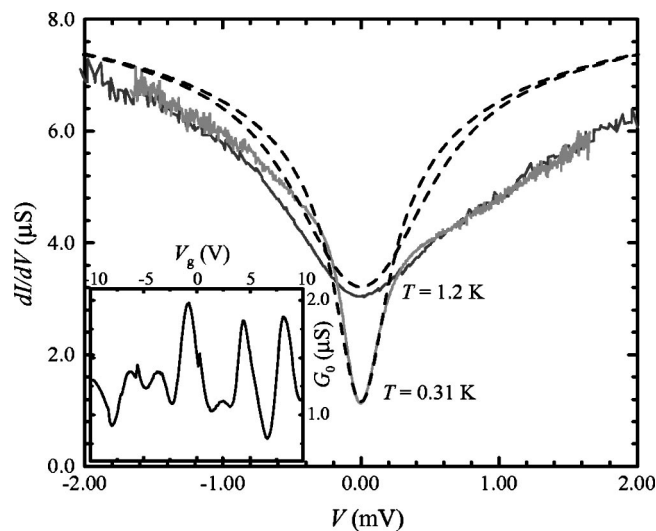


FIG. 2. G - V of sample A at two different temperatures. The dashed lines are theoretical curves calculated according to tunneling in an infinite 1D junction. Inset: Variation of the zero-bias conductance as a function of the back-gate voltage at $T=0.37$ K.

lower resistance, one-junction model is appropriate. Despite some irregular variation in the experimental G - V curves, which the theory does not account for, the theoretical curves are reasonable.

At higher bias voltages the conductance shows more irregular structure and may increase even nonmonotonously. The detailed characteristics for each sample are different. These features are less prominent on samples with more transparent contacts. Obviously it is not entirely correct to assume the transmission to be independent of energy. Such individual features may arise, e.g., from resonances in the transmission through the tunnel barriers,²⁴ and can be studied by shifting the Fermi level using a gate voltage (see inset to Fig. 2). This variation in conductance is similar in magnitude compared with the deviation of the experimental G - V curves from the theoretical prediction.

At small energies, $\epsilon \lesssim \hbar D^*/L_C^2$, the finite length of the contacts becomes significant, and the environment beyond the contact starts to determine the conductivity of the junction. In our samples, we estimate the cross-over temperature to be around 1 K, and the 1D model is found to be valid down to temperatures of that order [Fig. 1(b)]. The dimensional crossover from 1D to 0D is discussed in Ref. 14. Notably sample C shows deviation from the straight line behavior in plot of Fig. 1(b) towards low temperatures. However, extensive data from each regime would be necessary for a meaningful analysis of the crossover. It would be necessary to extend the measurements to temperatures below 0.3 K to show whether or not this crossover occurs as expected.

In the 0D regime, the LC -line environment is not a usable model, because our samples do not fulfill the condition $\epsilon > \hbar r/l$. Instead, one can use either a lumped resistor, or an RC -transmission line, which also incorporates the distributed capacitance c of the nanotube. The RC -transmission line is more accurate model for long nanotubes. Since in our samples the spacing of the electrodes is not much larger than their width, also finite length effects can come into play below 1 K. For very short tube segments, when $cL \ll C_T$, the difference between an RC -line and a lumped resistor model disappears.

Looking at Fig. 1(b), it appears that the straight line fit is less satisfactory for sample B than for the other samples. The temperature dependence is weaker than expected towards higher temperatures. If the data is plotted on $1/T$ scale instead of $1/\sqrt{T}$, as shown in Fig. 3, it becomes obvious that $G \propto \exp(-T_0/T)$ fits the data over a wider range in temperature than the 1D-tunnel junction model (dashed line in Fig. 3), which we have observed to hold in all our other samples. This type of temperature dependence suggests tunneling in a 0D junction. We have calculated theoretical temperature dependence and G - V curves using the EQFT¹⁶ and finite length RC -line model with $L=1$ μm . It turns out that the exact value of L is of no importance, but it provides a convenient low frequency cutoff. Results of the calculation are compared to the data both as a function of temperature (Fig. 3) and bias voltage [Fig. 4(a)], and a satisfactory fit is obtained. Just like in sample A, it is assumed that one of the junctions limits the conductivity and the other can be neglected (see schematic model in the inset to Fig. 3).

There are now three energy scales: The charging energy

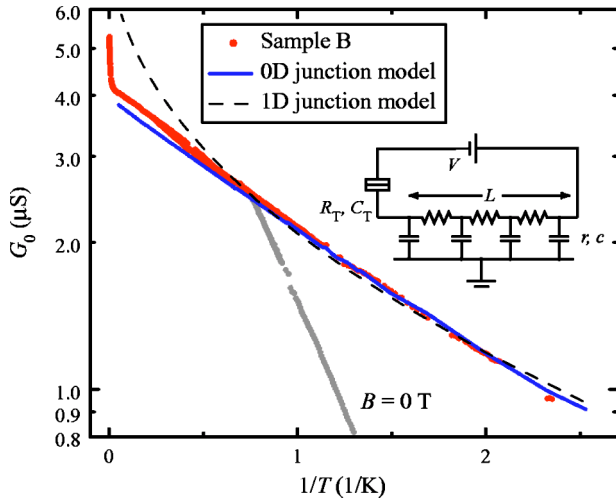


FIG. 3. (Color online) Conductance of sample B plotted on $1/T$ scale. The solid line results from a calculation using the EQFT for small tunnel junctions, with junction capacitance $C_T=260$ aF, $R_T=162$ k Ω , $r=45$ k $\Omega/\mu\text{m}$, and $c=240$ aF/ μm . The model is shown schematically in the inset. The dashed line is the calculation according to tunneling in an infinite 1D junction. In zero magnetic field, data has a sharp kink at T_C of the Al electrode.

$E_C=e^2/(2C_T)=3.6$ K, which is the most significant, ϵ^* as given in Eq. (3), but with c_T replaced by c , and, because of the finite length, the field Thouless energy $E_{\text{Th}}=\hbar D^*/L^2$. The fit depends only weakly on the exact value of ϵ^* (and therefore on r and c). In sample B, $E_C \gg E_{\text{Th}}$, and hence the transmission line is effectively infinite. Coulomb blockade is not due to two junctions in series, but due to the large resistance of the nanotube, $rL > R_Q$, which is enough to isolate an individual junction. Altogether there are four independent fitting parameters.

The reason why sample B shows 0D behavior in temperature range $T > 1$ K, where all the other samples are compatible with the 1D model, is possibly due to the character of the contacts. Even though the contacts appear wide on visual examination, it is possible that most of the current is conducted via a small part of the entire length, which would shift the 0D regime at $T \lesssim \hbar D^*/L_C^2$ towards higher temperatures.

As an additional check of the validity of the small junction model, the G - V curves for the superconducting electrode case were calculated. The additional parameter, the critical temperature $T_C=1.33$ K of Al, was taken as the point where zero bias conductance at zero magnetic field shows a sharp kink (Fig. 3). The calculation was repeated using the same parameters as for the normal case and BCS density of states in the superconducting Al electrode. Comparison to data [Fig. 4(b)] shows a satisfactory fit. Because the BCS theory is compatible with the suppression of conductivity when magnetic field is switched off, the tunneling contact must be located between the nanotube and one of the Al electrodes.

To conclude, we have measured the tunneling conductance in highly disordered MWNTs and observed that in most cases it obeys $G \propto \exp(-\sqrt{T_0}/T)$ instead of the power law, which is observed in the less disordered samples. This can be understood as a manifestation of tunneling into a 1D

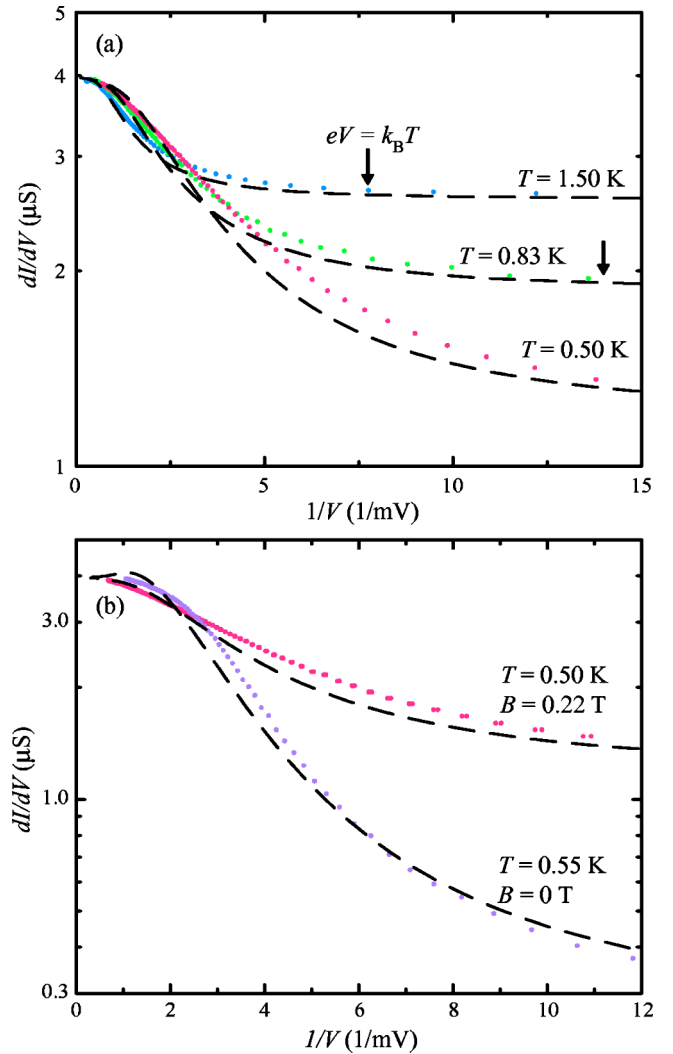


FIG. 4. (Color online) (a) Measured differential conductance at a few different temperatures on $1/V$ scale. The curves have been symmetrized by taking an average of the conductance on positive and negative bias voltages. The dashed lines are calculated from EQFT using the same parameters as in Fig. 3. (b) Differential conductance at zero and finite magnetic field, i.e., for superconducting and normal Al counterelectrodes.

disordered conductor. Similar suppression of tunneling DOS has been observed in a very long metallic 1D tunnel junction.¹⁷ However, in metallic systems the dip is small, only a few percent, due to the much higher conductivity of the electrodes, and therefore perturbation theory adequately accounts for the data. In our samples, it is possible to observe dips approaching 100% and the nonperturbative treatment becomes a must.

We thank A. Fonseca and J. Nagy from FUNDP, Namur for supplying us with the nanotubes. Useful discussions with J. Rollbühler, H. Grabert, and E. Sonin are gratefully acknowledged. This work was supported by the Academy of Finland and by the Large Scale Installation Program ULTI III of the European Union (Contract No. HPRI-1999-CT-00050).

*Electronic address: Reeta.Tarkiainen@hut.fi

†Permanent address: A. F. Ioffe Physical-Technical Institute, 194021 St. Petersburg, Russia.

- ¹S. Iijima, *Nature (London)* **354**, 56 (1991).
- ²M. Bockrath, D. H. Cobden, J. Lu, A. G. Rinzler, R. E. Smalley, L. Balents, and P. L. McEuen, *Nature (London)* **397**, 598 (1999).
- ³A. Bachtold, M. de Jonge, K. Grove-Rasmussen, P. L. McEuen, M. Buitelaar, and C. Schönenberger, *Phys. Rev. Lett.* **87**, 166801 (2001).
- ⁴E. Graugnard, P. J. de Pablo, B. Walsh, A. W. Ghosh, S. Datta, and R. Reifenberger, *Phys. Rev. B* **64**, 125407 (2001).
- ⁵R. Tarkiainen, M. Ahlskog, J. Penttilä, L. Roschier, P. Hakonen, M. Paalanen, and E. Sonin, *Phys. Rev. B* **64**, 195412 (2001).
- ⁶W. Yi, L. Lu, H. Hu, Z. W. Pan, and S. S. Xie, *Phys. Rev. Lett.* **91**, 076801 (2003).
- ⁷A. Kanda, K. Tsukagoshi, Y. Aoyagi, and Y. Ootuka, *Phys. Rev. Lett.* **92**, 036801 (2004).
- ⁸E. B. Sonin, *J. Low Temp. Phys.* **124**, 321 (2001).
- ⁹S. J. Tans, M. H. Devoret, H. Dai, A. Thess, R. E. Smalley, L. J. Geerligs, and C. Dekker, *Nature (London)* **386**, 474 (1997).
- ¹⁰L. Roschier, J. Penttilä, M. Martin, P. Hakonen, M. Paalanen, U. Tapper, E. I. Kauppinen, C. Journet, and P. Bernier, *Appl. Phys. Lett.* **75**, 728 (1999).
- ¹¹M. Ahlskog, R. Tarkiainen, L. Roschier, and P. Hakonen, *Appl. Phys. Lett.* **77**, 4037 (2000).
- ¹²A. Kanda, Y. Ootuka, K. Tsukagoshi, and Y. Aoyagi, *Appl. Phys. Lett.* **79**, 1354 (2001).
- ¹³B. L. Altshuler and A. G. Aronov, in *Electron-Electron Interaction in Disordered Systems*, edited by A. L. Efros and M. Pollak (North-Holland, Amsterdam, 1985).
- ¹⁴J. Rollbühler and H. Grabert, *Phys. Rev. Lett.* **87**, 126804 (2001).
- ¹⁵E. G. Mishchenko, A. V. Andreev, and L. I. Glazman, *Phys. Rev. Lett.* **87**, 246801 (2001).
- ¹⁶G.-L. Ingold and Y. V. Nazarov, in *Single Charge Tunneling*, edited by H. Grabert and M. H. Devoret (Plenum, New York, 1992), pp. 21–107.
- ¹⁷F. Pierre, H. Pothier, P. Joyez, N. O. Birge, D. Esteve, and M. H. Devoret, *Phys. Rev. Lett.* **86**, 1590 (2001).
- ¹⁸V. Krstić, S. Blumentritt, J. Muster, S. Roth, and A. Rubio, *Phys. Rev. B* **67**, 041401 (2003).
- ¹⁹D. Mendoza, F. Morales, and R. Escudero, *Solid State Commun.* **130**, 317 (2004).
- ²⁰K. Hernadi, A. Fonseca, J. B. Nagy, D. Bernaerts, A. Fudala, and A. A. Lucas, *Zeolites* **17**, 416 (1996).
- ²¹R. Tarkiainen, M. Ahlskog, A. Zyuzin, P. Hakonen, and M. Paalanen, *Phys. Rev. B* **69**, 033402 (2004).
- ²²L. G. Bulusheva, A. V. Okotrub, I. P. Asanov, A. Fonseca, and J. B. Nagy, *J. Phys. Chem. B* **105**, 4853 (2001).
- ²³R. Tarkiainen, M. Ahlskog, P. Hakonen, and M. Paalanen, *Physica E (Amsterdam)* **18**, 206 (2003).
- ²⁴J. J. Palacios, A. J. Pérez-Jiménez, E. Louis, E. San Fabián, and J. A. Vergés, *Phys. Rev. Lett.* **90**, 106801 (2003).